HHS Public Access

Author manuscript

Nat Cell Biol. Author manuscript; available in PMC 2010 July 01.

Published in final edited form as:

Nat Cell Biol. 2010 January ; 12(1): 41–8. doi:10.1038/ncb2002.

Sec24b selectively sorts Vangl2 to regulate planar cell polarity during neural tube closure

Janna Merte[1,*], **Devon Jensen**[2,*], **Kevin Wright**[1], **Sarah Sarsfield**[1], **Yanshu Wang**[3], **Randy Schekman**[2], and **David D. Ginty**[1,4]

[1]The Solomon H. Snyder Department of Neuroscience and Howard Hughes Medical Institute, Johns Hopkins University, Baltimore, MD 21205

[2]Department of Molecular and Cell Biology and Howard Hughes Medical Institute, University of California at Berkeley, Berkeley, CA 94720

[3]Department of Molecular Biology and Genetics and Howard Hughes Medical Institute, Johns Hopkins University, Baltimore, MD 21205

Abstract

Craniorachischisis is a rare but severe birth defect that results in a completely open neural tube. Mouse mutants in planar cell polarity (PCP) signaling components have deficits in the morphological movements of convergent extension (CE) that result in craniorachischisis. Using a forward-genetic screen in mice, we have identified Sec24b, a cargo-sorting member of the core complex of the COPII endoplasmic reticulum (ER)-Golgi transport vesicle, as critical for neural tube closure. *Sec24b*^{Y613} mutants exhibit craniorachischisis, deficiencies in CE, and other PCP-related phenotypes. Vangl2, a key component of the PCP-signaling pathway critical for CE, is selectively sorted into COPII vesicles by Sec24b. Moreover, *Sec24b*^{Y613} genetically interacts with a loss-of-function *Vangl2* allele (*Vangl2*^{LP}) causing a marked increase in the prevalence of spina bifida. Interestingly, the Vangl2 looptail point mutants D255E and S464N, known to cause defects in CE, fail to sort into COPII vesicles and are trapped in the ER. Thus, during COPII vesicle formation, Sec24b exhibits cargo specificity for a core PCP component, Vangl2, the proper ER to Golgi transport of which is essential for the establishment of PCP, convergent extension, and closure of the neural tube.

[4]Correspondence should be addressed to DDG: dginty@jhmi.edu.

[*]These authors contributed equally to this work

Author Contributions: JM and DDG designed the forward genetic screen. JM developed and implemented the screen, identified the novel mouse line with craniorachischisis, did the positional cloning to map the mutation to *Sec24b*^{Y613}, characterized PCP-related phenotypes in the *Sec24b*^{Y613} mutants, and showed that *Vangl2*^{LP} and *Sec24b*^{Y613} genetically interact. DJ did the experiments showing that Sec24b^{Y613} cannot form an oligomer with Sec23, and the COPII vesicle sorting experiments showing that Vangl2 is selectively sorted by Sec24b and that mutant forms of Vangl2 fail to properly sort into these vesicles. KW identified and analyzed the missexpression of Vangl2 in *Sec24b*^{Y613} mutant neuroepithelium. YW aided in experimental planning of PCP phenotype analysis and performed some cochlear hair cell orientation analysis. SS aided in the implementation of the forward genetic screen that identified *Sec24b*^{Y613} and the mapping of the point mutation. RS provided experimental design and analysis of the role of Sec24b in the sorting and expression of Vangl2 and Vangl2 mutant proteins. DDG provided experimental design and analysis of the forward-genetic screen, mutation mapping, and mouse phenotypic analysis. JM and DDG wrote the manuscript.

The authors declare they have no competing interests.

Neural tube closure defects result from fundamental failures of developmental processes during neurulation. Most common among these disorders is spina bifida, a failure of caudal tube closure, and anencephaly, a failure of rostral neural tube closure. A rare disorder, craniorachischisis, is a closure failure along the entire anterior-posterior axis from the midbrain-hindbrain boundary to the most caudal end of the neural tube. During neurulation in the mouse, the neural plate undergoes several morphological changes: neural folds are created, migrate toward the midline, and eventually fuse. As migratory cells intercalate with each other, the embryo is lengthened at the expense of the width within the medial-lateral plane in a process called convergent extension (CE). The first neural tube closure event (closure 1) begins at the boundary between the hindbrain and the cervical region and spreads both rostrally and caudally into the hindbrain and developing spinal cord, respectively. Thus, when closure 1 fails, the entire neural tube from the midbrain to the caudal neural tube remains open resulting in craniorachischisis[1, 2].

Currently, all known mutations that result in craniorachischisis in the mouse have been mapped to the vertebrate orthologs of components of the planar cell polarity (PCP) pathway, first identified for its role in tissue patterning of the fly[1, 2]. Loss-of-function mutations in *Vangl2*[3, 4], *Fzd*, (*Fzd3;Fzd6* double mutants[5]), *Celsr1*[6], *Dvl* (*Dvl1;Dvl2* double mutants[7, 8]) as well as *Ptk7*[9] and *Scribble*[10, 11] all cause craniorachischisis in the mouse, indicating that the non-canonical Wnt signaling pathway is critical for developmental events underlying the initiation of closure 1 during neurulation. Craniorachischisis in these mutants results from deficits in CE during the migratory movements required to initiate closure 1[12-14].

Using a three-generation, forward-genetic screen for recessive mutations affecting neural development[15] (Supplemental Figure 1) we identified mouse line 811. Mutant 811 mice were easily distinguished from their littermates, as homozygous mutants within this allelic group developed craniorachischisis (Figure 1A). This mutant allele was found to segregate with Mendelian ratios with 48% (129/267) of parents carrying the allele and 12% (1/4 affected × 1/2 females are carriers) of embryos (232/1984) displaying the fully open neural tube (Supplemental Figure 2). By embryonic day 18.5 (E18.5), approximately 33% of the mutants isolated were dead or dying but could still be scored and genotyped.

The genetic lesion underlying the craniorachischisis observed in line 811 was mapped to a 1.8 Mb region of chromosome 3 between rs13477397 and rs1347704 that contained 17 open reading frames. We sequenced the exons containing 5′UTR and coding sequence for the 14 loci without existing mouse models (Supplemental Methods; Figure 1B). This sequence analysis revealed a single base pair substitution within all of the sequences analyzed. This point mutation was a T>A transversion in exon 9 of *Sec24b*. Two different transcript variants can be processed from the *Sec24b* locus of the mouse: *ENMUST00000001079*/ *NCBI (1079)* and *ENMUST00000098616 (98616)* (Figure 1C, exon 9 highlighted in red). The T>A transversion is 2078T>A in *1079* and 1834T>A in *98616* (Figure 1D). The nucleotide substitution results in truncated proteins, Sec24b Y613 and Sec24b Y578 in 1079 and 98616, respectively (Figure 1E). Confirmation that the neural tube closure phenotype associated with line 811 is caused by the mutation in *Sec24b* (*Sec24b*^{Y613}) is provided by a second independently identified mouse mutant that harbors a distinct loss-of-function mutation in *Sec24b* (*Sec24b*^{S135X}) and also exhibits chraniorachischisis (Frits Meijlink,

Hubrecht Institute, Netherlands, personal communication). Sec24b is one of four mammalian orthologs of the yeast Sec24, and the first vertebrate Sec24 to be characterized *in vivo*.

Sec24b functions as a cargo-binding component of the COPII vesicle coat[16-19]. These COPII vesicles are the primary pathway for active transport of secretory proteins from the ER to the Golgi. Thus, as an initial step in the forward secretion of nearly all non-ER-resident membrane and luminal proteins, COPII-mediated vesicle transport plays a key role in enabling the proper cellular localization of thousands of proteins. Sec23, the GTPase activating member of the complex, and Sec24 components form tight heterodimers in the cytosol, and this complex is then recruited to sites of active COPII budding – termed ER exit sites. Once recruited to the ER membrane, Sec24 proteins package cargo into the vesicle at sites of active budding. Based on co-crystal structural studies[20], it appears that Sec24b Y613 is truncated prior to the putative Sec23 binding site. Therefore, we predicted that Sec24b Y613 would lose its ability to associate with its Sec23 binding partners, rendering it functionally inactive. Indeed, we found that in contrast to wildtype Sec24b, mutant Sec24b Y613 failed to co-immunoprecipatate with either Sec23a or Sec23b in heterologous cells and was not concentrated at ER exit sites marked by another COPII component, Sec13 (Supplemental Figure 3). Thus, *Sec24b*^{Y613} functions as a loss-of-function allele encoding a protein that is incapable of associating with other components of the COPII complex and is not recruited to ER exit sites.

Given that other mouse mutants with craniorachischisis have deficits in CE[12, 14, 21], we analyzed the embryonic morphology of *Sec24b* mutants during neurulation prior to neural tube closure. To do this, we examined *Sec24b*$^{Y613/Y613}$ mutants and control littermates at E8.5 for deficits in the length: width ratio. A decrease in this ratio reflects a developmental failure in the migratory movements required to lengthen the embryo and facilitate midline fusion[14]. At the 6-, 7-, 8-, and 10-somite stages, *Sec24b*$^{Y613/Y613}$ mutants were shorter and wider than littermates, confirming a deficit in the morphogenic movements of CE (Figure 2A). These finding indicate that the developmental events underlying craniorachischisis in *Sec24b*^{Y613} mutants are shared with other mouse mutants in the PCP-signaling pathway.

CE-deficient craniorachischisis is common to mouse mutants with deficits in the PCP-signaling pathway; thus, we sought to determine if other PCP-dependent phenotypes were also found in *Sec24b*$^{Y613/Y613}$ embryos. First, all mutants isolated at E18.5 were scored for omphalocele, a congenital birth defect in which the intestines, liver, and occasionally other organs develop outside of the abdomen because the tissues of the abdominal wall fail to fuse at the midline. We observed omphalocele in 45% (n=38) of the late gestation mutant embryos but in fewer than 1% (n=166) of littermate controls. Second, we examined the fusion of the eyelids in all of the E18.5 *Sec24b*$^{Y613/Y613}$ embryos. In nearly all of these mutants (99%, n=38), the upper and lower eyelids failed to fuse. In contrast, eyelid fusion failure was observed in only 2% (n=166) of littermate controls (Figure 2B).

Defects in the orientation of sensory hair cells of the cochlea and the vestibular system are also frequently observed in mice lacking core PCP components[22]. Using immunological techniques to label the cilia of hair cells within these tissues, we examined the orientation of

hair cells of the cochlea and vestibular system. In the cochlea, *Sec24b*$^{Y613/Y613}$ embryos exhibited deficits in the orientation of both the outer and inner hair cells. In addition, the alignment of both the outer and inner hair cells of the cochlea was abnormal in *Sec24b*$^{Y613/Y613}$ embryos with hair cells periodically falling out of phase from the row (Figure 2C). This defect was present across the entire organ of Corti. However, no differences between the *Sec24b*$^{Y613/Y613}$ mutants and littermate controls with respect to the orientation of hair cells in the vestibular system were observed. In addition, we examined the orientation of hair follicles of the back skin in *Sec24b*$^{Y613/Y613}$ embryos and their littermate controls. Hair follicle orientation of the mutants at this stage appeared relatively normal (data not shown). Therefore, in addition to craniorachischisis, *Sec24b*$^{Y613/Y613}$ mutants share most of the phenotypic characteristics of mice harboring mutations within components of the core PCP-signaling complex indicating that Sec24b might function by interacting with a component of the PCP pathway.

The role of Sec24b in the formation of COPII vesicles destined to transit between the ER and Golgi and the PCP-signaling dependent phenotypes found in *Sec24b*$^{Y613/Y613}$ mutants indicate that Sec24b Y613 might fail to properly sort and traffic a known member of the core PCP complex. Of the mouse mutants displaying craniorachischisis, five alleles code for proteins that are trafficked through the secretory pathway: Vangl2, Celsr1, Ptk7, Fzd6, and Fzd3. Of these genes, *Vangl2* is the only dosage sensitive allele. Loss-of-function *Vangl2* (*Vangl2*^{LP}) heterozygotes have partial deficits with respect to neural tube closure that result in the looped-tail phenotype[23]. Moreover, the *Vangl2*^{LP} allele genetically interacts with other members of the PCP signaling complex[9, 10, 24].

Given the functional centrality of Vangl2 in PCP signaling as well as the dosage sensitivity of *Vangl2*^{LP} mice[23], we tested for a genetic interaction between *Sec24b* and *Vangl2* by crossing *Vangl2*$^{+/LP}$ mice with *Sec24b*$^{+/Y613}$ mice to create *Vangl2*$^{+/LP}$*; Sec24b*$^{+/Y613}$ embryos. In litters collected between E13.5 and E18.5, approximately 5% (n=40) of the *Vangl2*$^{+/LP}$; *Sec24b*$^{+/+}$ embryos had a caudal neural tube closure defect. In striking contrast, 68% (n=18) of *Vangl2*$^{+/LP}$*; Sec24b*$^{+/Y613}$ embryos exhibited spina bifida. No littermates of other genotypes displayed this defect (Figure 3). In addition, between late embryogenesis and four weeks of age, over 50% of the *Vangl2*$^{+/LP}$*; Sec24b*$^{+/Y613}$ mice died. The strong genetic interaction between *Sec24b* and *Vangl2* suggests that Sec24b might directly regulate the trafficking and cell surface expression of Vangl2 during development.

Many transmembrane proteins are likely sorted into COPII vesicles via cargo binding sites common among all Sec24 proteins[19]. However, the conservation of four distinct vertebrate paralogs suggests that each Sec24 may have evolved the ability to transport specific and essential cargos. To establish a direct measure of the ER export of Vangl2 and to assess the role of Sec24b in the trafficking of Vangl2, we used an *in vitro* vesicle budding reaction[25]. Using this assay, Vangl2-containing vesicles were formed in a COPII-dependent manner. More importantly, reactions supplemented with recombinant Sec24b, but not with the other Sec24 paralogs, substantially increased the amount of Vangl2 packaged into COPII vesicles. In contrast, another known COPII cargo protein Amyloid Precursor Protein (APP), which is packaged and transported in a COPII dependent manner, showed no specificity for any of

the Sec24 paralogs (Figure 4A). Thus, Vangl2 is preferentially sorted by Sec24b during COPII vesicle formation from the ER.

Two semi-dominant, loss-of-function alleles of Vangl2 have been mapped and isolated using classical genetics: *Vangl2*^{LP} (S464N)[10] and *Vangl2*$^{Lp\text{-}m1Jus}$ (D255E)[3]. Heterozygotes of both alleles exhibit a looped-tail phenotype whereas homozygous mutants exhibit craniorachischisis. Both point mutations map to the cytosolic C-terminal domain of Vangl2 and could inhibit the ability of Vangl2 to interact with COPII or other cytosolic chaperones. Therefore, we assessed the ability of Vangl2 looptail mutant proteins to be packaged into COPII vesicles using the *in vitro* vesicle budding assay. As before, Vangl2 was packaged into vesicles in a COPII dependent manner, but strikingly, neither Vangl2 S464N nor D255E was capable of entering COPII vesicles (Figure 4B). This effect was especially surprising given the conservative D255E substitution found in the *Vangl2*$^{Lp\text{-}m1Jus}$ allele. Neither mutation depressed COPII budding, as other cargo proteins were still packaged normally (Supplemental Figure 4). Correspondingly, Vangl2 D255E and S464N co-localize with Protein Disulfide Isomerase (PDI), an ER marker, and fail to reach the plasma membrane (Figure 4C).

Our findings suggest that the loss-of function phenotypes observed in *Sec24b*$^{Y613/Y613}$, *Vangl2*^{LP} and *Vangl2*$^{Lp\text{-}m1Jus}$ mice result from trafficking defects in which the Vangl2 protein fails to package into COPII vesicles and exit the ER and are consistent with other studies showing a lack of Vangl2 plasma membrane localization in Vangl2^{LP} mutants[26]. To further test this idea, we used immunohistochemistry to analyze the subcellular localization of Vangl2 in the developing neural tube of both *Sec24b*$^{Y613/Y613}$ and *Vangl2*^{LP} mutant mice. As a control, the subcellular localization of Beta-catenin, a membrane bound protein not associated with the PCP pathway, was assessed in the same tissue. Vangl2 protein was mislocalized to puncta within the cytoplasm of *Sec24b*$^{Y613/Y613}$ mutants while Vangl2 co-localized with Beta-catenin at the plasma membrane in wildtype embryos (Figure 5). As previously reported[26], Vangl2 trafficking to the plasma membrane in *Vangl2*^{LP} mutants was aberrant (Figure 5). In contrast, the pattern of subcellular distribution of Fzd3 in cells of the neural tube is comparable in wildtype, *Sec24b*$^{Y613/Y613}$, *Vangl2*^{LP} mice (Supplemental Figure 5). These results are consistent with our *in vitro* findings showing that Vangl2 is selectively sorted by Sec24b during COPII vesicle formation. Most fundamentally, these data indicate that Sec24b is essential for proper membrane localization of Vangl2 *in vivo*.

Here, we have identified Sec24b as a critical regulator of planar cell polarity signaling. In addition to the severe craniorachischisis phenotype, *Sec24b*^{Y613} mutants have several other phenotypic abnormalities common to mouse mutants in components of the core PCP complex. Sec24b regulates cell surface expression of the dosage-dependent, core PCP protein Vangl2 by preferentially sorting this cargo into COPII vesicles. Additionally, Vangl2 looptail mutations prevent Vangl2 from being packaged into COPII vesicles and exiting the ER. Thus, it is likely that insufficient Vangl2 is brought to the cell surface during neurulation in *Sec24b* or *Vangl2* mutants. This mislocalization of Vangl2 disrupts the entire PCP signaling cascade, resulting in a neural tube closure deficit similar to that observed in null alleles of other components of the core PCP complex. It is noteworthy that mice that are heterozygous for both *Sec24b*^{Y613} and *Vangl2*^{LP} have a propensity to develop spina bifida.

Given that most human genetic diseases are not recessive but rather arise from the interactions of multiple loci, human mutations in *Sec24b* are likely to contribute to spina bifida.

Our analysis of Sec24b Y613 identifies a novel mechanism of protein regulation during development. Sec24b is one of four paralogs that function in the trafficking of secretory proteins between the ER and Golgi. Thus, loss of Sec24b function would be predicted to lead to deficits in the cell surface expression of some transmembrane proteins. *Sec24b* mutants, though clearly developmentally abnormal for neural tube closure, are relatively spared with respect to many other developmental processes. Vangl2 may be one of a small set of COPII cargo proteins whose expression is strictly dependent on Sec24b. Nonetheless, our findings indicate that cargo specificity has evolved between the four Sec24 paralogs with Sec24b being specifically required for trafficking of a core PCP component, Vangl2, and the establishment of planar cell polarity, convergent extension and neural tube closure.

Methods

Mutagenesis

C57BL/6 (BL6) mice were injected with ENU as described [27-29]. Briefly, BL6 male mice were injected with 3×100mg/kg body weight ENU to induce random mutations throughout the genome. Using a three-generation forward-genetic screen, we outbred and isolated the mutations in C3H/He mice to facilitate mapping by polymorphism. Resulting G1 fathers were mated to their G2 daughters and embryos were screened for developmental anomalies (Supplemental Figure 1).

Mapping

The genetic lesion responsible for craniorachischisis in line 811 was mapped via backcross (Supplemental Figure 3) using standard linkage analysis with a panel of PCR polymorphisms between C57BL/6 (BL6) and C3H/He (C3H) mice (Supplemental Table 1) to the distal end of chromosome 3. Analyses at several other polymorphisms placed 811 within a 3.7Mb region between D3MIT319 and D3MIT254. We analyzed the D3MIT319 recombinants (10/527) at rs13477397, rs4231957, and rs13477402 and found recombination at rs13477397 (9/531) but not at rs4231957 or rs13477402. Likewise, we analyzed the recombinants at D3MIT254 (3/509) at rs13477404 and rs13477406 as well as rs4231957 and rs13477402 and identified a single recombination event that spanned D3MIT254 through rs13477404. Thus, 811 was determined to be in the 1.8 Mb region between rs13477397 and rs1347704 containing 17 open reading frames. Of these 17 predicted genes, 3 had mouse models that did not exhibit craniorachischisis and could be eliminated. We sequenced the exons containing 5′UTR and coding sequence for all of the 14 remaining loci (*ENSMUSG00000074236*, *Elov6*, *ENSMUSG00000080139*, *ENSMUSG00000068627*, *Rrh*, *Nola1*, *Cfi*, *Pla2g12a*, *9030408N13Rik (Ccdc109b)*, *Sec24b*, *Rpl12*, *Col25a1*, *ENSMUSG00000065788*) using DNA isolated from two mutants and one BL6 control mouse. Several of these genes were sequenced by the Harvard University Partners Genomics Facility.

Genotyping

Sec24b^{Y613} creates a restriction enzyme-sensitive polymorphism. This line is genotyped by amplification of an approximately 200 bp fragment with TCAAACACCATCGTGAGGTGCC and ACCCGAAACTCACCATCAATAACT, followed by subsequent digestion with MseI.

Convergent extension

Mutants and controls from E8.5 litters were isolated and then binned based on somite number. The length and width of each embryo was then quantified, the length:width ratio calculated, the embryos were then genotyped and the length:width ratio compared between mutants and controls by ANOVA followed by Student Newman-Keuls post hoc. n=7, 8, 7, 9 mutants at the 6-, 7-, 8-, and 10-somite stages, respectively.

Immunohistochemisty

E18.5 mouse cochlea staining was performed as described[5]. Staining of E10.5 spinal cords was performed as described with minor modifications[26]. Embryos were fixed in 2% paraformaldehyde, washed twice in PBS, embedded in OCT and frozen. 10μM sections were collected on slides and antigen retrieval was performed by incubating the slides in Sodium Citrate Buffer (10 mM Sodium Citrate, 0.05% Tween-20, pH 6.0) for 30 minutes at 95° C. Slides were washed three times in PBS and incubated overnight at 4°C with PBS containing anti-Vangl2 (1:150), anti-B-Catenin (1:250), and/or anti-Fzd-3 (1:50), 10% normal goat serum and 0.4% Triton-×100. The following day, slides were washed and incubated with the appropriate fluorescent secondary antibodies (1:400) for 4 hours at room temperature.

In Vitro COPII vesicle budding assay

Procedure for making cell free mRNA, semi-intact cells, and subsequent *in vitro* translation was preformed as described[25], [30] with some modifications. The vesicle formation reaction and vesicle purification procedure was essentially as described[31], with some modifications. In detail, COS7 cells grown in 3×100mM plates were washed in PBS, removed from plates with trypsin, and washed again in PBS containing 10μg/ml soybean trypsin inhibitor. Then, cells were permeablized with 40μg/ml digitonin for 5 minutes in ice-cold KHM buffer (110 mM KOAc, 20 mM Hepes, pH 7.2, and 2 mM $Mg(OAC)_2$) and washed and resuspended in 100μl KHM. Endogenous RNA was degraded after addition of 1mM $CaCl_2$ and 10μg/ml micrococcal nuclease and incubation at room temperature for 12 minutes. After incubation, the nuclease reaction was stopped by addition of 4mM EGTA, and cells were pelleted and washed. Semi-intact RNA-free cells were resuspended in KHM buffer such that the measurement of absorbance (600 nm) for 5μl of cells in 500μl KHM was 0.08. These cells were added to an *in vitro* translation reaction with rabbit reticulocyte lysate (Promega, Flexi®) and RNA encoding HA-Vangl2, which was incubated for 60 minutes at 30°C. Then, these donor membranes were washed to remove non-translocated protein products and resuspended in KHM.

To form vesicles, donor membranes with newly synthesized HA-Vangl2 were combined where indicated with rat liver cytosol, ATP regenerating system (40 mM creatine phosphate,

0.2 mg/ml creatine phosphokinase, and 1 mM ATP), 0.2 mM GTP and/or recombinant COPII proteins, followed by incubation at 30°C for 1 hour. Newly formed vesicles were separated from the more rapidly sedimenting donor membranes by centrifugation at 13000*xg* for 12 minutes. Vesicles were collected by centrifugation at 115000*xg* for 25 minutes. Vesicle pellets were resuspended and washed in 100μl cold KHM, centrifuged again, and finally solubilized in 16 μl of Buffer C (10 mM Tris-HCl (pH 7.6), 100 mM NaCl, 1% Triton X-100 plus protease inhibitor mixture) and Laemmli sample buffer. Vesicle fractions and original donor membranes were resolved on SDS-PAGE, transferred onto PVDF membranes, and subjected to immunoblot to detect HA-Vangl2 and the positive control endogenous cargo proteins, Amyloid Precursor Protein, ERGIC-53 and Sec22.

Antibodies

Anti-Sec13 antiserum was raised in rabbits injected with a purified recombinant His-tagged human full length Sec13 produced in baculovirus-infected SF9 cells. Anti-Sec22 antiserum was raised in rabbits injected with the peptide (CG)-HSEFDEQHGKKVPTVSRPYSFIEFDT (residues 91-116) conjugated to rabbit serum albumin. Anti-HA was purchased from Covance (16B12). Anti-Myc was purchased from Cell Signaling Technologies (2276). Anti-Flag and Anti-Amyloid Precursor Protein were purchased from Sigma (F3165 and A8717, respectively). Monoclonal anti-Protein Disulfide Isomerase was a gift from S. Fuller (EMBL-Heidelberg). Anti-ERGIC-53/LMAN-1/p58 antiserum was generated as described[32]. Anti-Vangl2 was a gift from P. Gros and anti-Fzd-3 was a gift from J. Nathans. Anti-Beta-Catenin was purchased from Cell Signaling Technologies (2677). Anti-mouse and Anti-rabbit HRP conjugates were purchased from GE Healthcare UK (NXA931 and NA934V, respectively). Anti-mouse FITC conjugate and Anti-rabbit TRITC conjugate were both purchased from Jackson ImmunoResearch (715-095-151 and 711-025-152, respectively).

Immunofluorescence

COS7 cells grown on coverslips were transiently transfected with plasmids encoding 3×HA-Vangl2 WT, Lp255, or Lp464 or 6×Myc-Sec24b WT or Y613 using Lipofectamine 2000 and the manufacturer's recommended protocol. Twenty hours later, cells were processed by immunofluorescence. All subsequent steps were at room temperature and all washing steps used 3 changes of 2ml PBS. Cells on coverslips were fixed in 2.5% paraformaldehyde for 15 minutes and washed. Next, they were permeablized in 0.1% Trition X-100 in PBS for 1 minute and washed. The cells were then blocked with 1% BSA in PBS for 30 minutes. Next, cells on coverslips were incubated with the indicated primary antibodies diluted in 1% BSA for 1 hour and washed. Then, they were incubated in secondary anti-rabbit or anti-mouse fluorescent conjugates diluted in 1% BSA for 1 hour and washed. Finally, coverslips were briefly incubated in 1ug/ml DAPI and were mounted on glass slides in mowiol mounting medium. Cells were imaged using a Zeiss AxioObserver Z1 fluorescent microscope and images were captured and merged with Metamorph software from Molecular Devices.

Immunoprecipatations

COS7 cells grown in wells of a 6-well plate were transiently transfected with 6×Myc-Sec24b WT or Y613, and with Flag-Sec23a or Flag-Sec23b, using Lipofectamine 2000 and the manufacturer's recommended protocol. Twenty-four hours later, cells were washed 2 times in PBS. Then, cells were solubilized in 200μl of RIPA buffer (1% Triton X-100, 1% sodium deoxycholate, 0.1% SDS, 0.15 M NaCl, 0.01 M Na_2PO_4, protease inhibitor mixture, pH 7.2). Cell lysates were cleared by centrifugation at 15000*xg* for 10 minutes and the supernatant was transferred to a new tube. A 20μl sample of input lysate was reserved in a separate tube and mixed with Buffer C and Laemmli sample buffer. Primary anti-Myc antibody was added to a concentration of 1:300 and rotated at 4°C for 3 hours. Then, 40μl of 50% slurry washed Protein A-sepharose beads was added and the lysate was again rotated at 4°C for 2 hours. Beads were pelleted at 2000*xg* and washed 4 times in RIPA buffer. The beads were resuspended in 80 μl of Buffer C and 2× Laemmli sample buffer. Finally, samples were resolved on SDS-PAGE, transferred onto PVDF membranes, and subjected to immunoblot to detect Myc-Sec24b and Flag-Sec23.

Recombinant protein purification

Recombinant human Sar1 H79G was overexpressed in E. Coli and purified as previously described[31]. Human Flag-Sec23a/His-Sec24a, Flag-Sec23a/His-Sec24b, Flag-Sec23a/His-Sec24c, and Flag-Sec23a/His-Sec24d were expressed in SF9 cells using a baculovirus system and purified as previously described[31].

Materials

Rabbit muscle creatine phosphokinase, creatine phosphate, ATP, GTP and protease inhibitor mixture tablets were purchased from Roche Applied Science. Protein A-sepharose was purchased from BioVision. Rat liver cytosol was prepared as previously described[31]. Trypsin 0.05% with EDTA was purchased from Invitrogen. Soybean trypsin inhibitor was purchased from Fluka Biochemika. Micrococcal nuclease from Staphylococcus aureus was purchased from USB-Affymetrix, dissolved in 50mM glycine, 5mM $CaCl_2$ pH 9.2 and stored in 1mg/ml aliquots. Digitonin was purchased from Sigma and dissolved in DMSO at 40mg/ml.

Plasmids

3×HA-Vangl2 Lp255 and Lp464 were created using site-directed mutagenesis on the pCS2 3×HA-Vangl2 WT plasmid according to the QuikChange protocol from Stratagene, using respective primers: 5′-GTCGTGCGATCCACAGAAGGGGCCAGC-3′ + 5′-GCTGGCCCCTTCTGTGGATCGCACGAC-3′ or 5′-AAACAGTGGACCTTGGTGAACGAGGAGCCG-3′ + 5′-CGGCTCCTCGTTCACCAAGGTCCACTGTTT-3′. F l a g-Sec23a and Flag-Sec23b mammalian expression vectors were created by amplifying the tagged ORF from separate baculovirus plasmids, pFastBac-Flag-Sec23a and pFastBac-Flag–Sec23b (9), using primers: 5′-GCGCGGATCCATGGACTACAA-3′ (both forward) and 5′-TCTCGGCGCGCCTCAAGCAGCACTGGACACAGC-3′ or 5′-TCTCGGCGCGCCTTAACAGGCACTGGAGACAGCC-3′ (reverse, respectively). Then,

the tagged ORFs were inserted into BamHI and AscI restriction sites of the mammalian expression plasmid pCS2.

Supplementary Material

Refer to Web version on PubMed Central for supplementary material.

Acknowledgments

We thank Jeremy Nathans, Takako Makita, Alex Kolodkin, and members of the Ginty laboratory for discussions and reading and commenting on this manuscript. We thank Philippe Gros for providing the Vangl2 antibody. We thank J.C. Fromme, B. Kleizen, and A. Schindler for Anti-Sec13 and Anti-Sec22 antiserum and C.Chan for recombinant Sec23A/Sec24A and Sec23A/Sec24C. For excellent technical help we thank B. Yang and Y. Wu. Experiments in this manuscript were funded by NIH grants NS34814 (DDG) and the Johns Hopkins Mind Brain Institute. DDG and RS are investigators of the Howard Hughes Medical Institute.

References

1. Kibar Z, Capra V, Gros P. Toward understanding the genetic basis of neural tube defects. Clin Genet. 2007; 71:295–310. [PubMed: 17470131]
2. De Marco P, Merello E, Mascelli S, Capra V. Current perspectives on the genetic causes of neural tube defects. Neurogenetics. 2006; 7:201–221. [PubMed: 16941185]
3. Kibar Z. Identification of a New Chemically Induced Allele (Lpm1Jus) at the Loop-Tail Locus: Morphology, Histology, and Genetic Mapping. Genomics. 2001; 72:331–337. [PubMed: 11401449]
4. Montcouquiol M, et al. Identification of Vangl2 and Scrb1 as planar polarity genes in mammals. Nature. 2003; 423:173–177. [PubMed: 12724779]
5. Wang YNG, Nathans J. The Role of Frizzled3 and Frizzled6 in Neural Tube Closure and in the Planar Polarity of Inner-Ear Sensory Hair Cells. J Neurosci. 2006; 26:2147–2156. [PubMed: 16495441]
6. Curtin J. Mutation of Celsr1 Disrupts Planar Polarity of Inner Ear Hair Cells and Causes Severe Neural Tube Defects in the Mouse. Current Biology. 2003; 13:1129–1133. [PubMed: 12842012]
7. Hamblet N, et al. Dishevelled 2 is essential for cardiac outflow tract development, somite segmentation and neural tube closure. Development. 2002; 129:5827–5838. [PubMed: 12421720]
8. Etheridge SL, et al. Murine dishevelled 3 functions in redundant pathways with dishevelled 1 and 2 in normal cardiac outflow tract, cochlea, and neural tube development. PLoS Genet. 2008; 4:e1000259. [PubMed: 19008950]
9. Lu X, et al. PTK7/CCK-4 is a novel regulator of planar cell polarity in vertebrates. Nature. 2004; 430:93–98. [PubMed: 15229603]
10. Murdoch J, et al. Circletail, a New Mouse Mutant with Severe Neural Tube Defects: Chromosomal Localization and Interaction with the Loop-Tail Mutation. Genomics. 2001; 78:55–63. [PubMed: 11707073]
11. Murdoch J, et al. Disruption of scribble (Scrb1) causes severe neural tube defects in the circletail mouse. Human Molecular Genetics. 2003; 12:87–98. [PubMed: 12499390]
12. Ybot-Gonzalez P, et al. Convergent extension, planar-cell-polarity signalling and initiation of mouse neural tube closure. Development. 2007; 134:789–799. [PubMed: 17229766]
13. Mlodzik M. Planar cell polarization: do the same mechanisms regulate Drosophila tissue polarity and vertebrate gastrulation? Trends Genet. 2002; 18:564–571. [PubMed: 12414186]
14. Wallingford J, Fraser SE, Harland RM. Convergent extension: the molecular control of polarized cell movement during embryonic development. Developmental Cell. 2002; 2:695–706. [PubMed: 12062082]
15. Kasarskis A, Manova K, Anderson KV. A phenotype-based screen for embryonic lethal mutations in the mouse. Proc Natl Acad Sci U S A. 1998; 95:7485–7490. [PubMed: 9636176]
16. Wendeler M, Paccaud J, Hauri H. Role of Sec24 isoforms in selective export of membrane proteins from the endoplasmic reticulum. EMBO Rep. 2007; 8:258–264. [PubMed: 17255961]

17. Shimoni Y, et al. Lst1p and Sec24p cooperate in sorting of the plasma membrane ATPase into COPII vesicles in Saccharomyces cerevisiae. J Cell Biol. 2000; 151:973–984. [PubMed: 11086000]
18. Miller E, Antonny B, Hamamoto S, Schekman R. Cargo selection into COPII vesicles is driven by the Sec24p subunit. EMBO J. 2002; 21:6105–6113. [PubMed: 12426382]
19. Miller EA, et al. Multiple cargo binding sites on the COPII subunit Sec24p ensure capture of diverse membrane proteins into transport vesicles. Cell. 2003; 114:497–509. [PubMed: 12941277]
20. Bi X, Corpina RA, Goldberg J. Structure of the Sec23/24-Sar1 pre-budding complex of the COPII vesicle coat. Nature. 2002; 419:271–277. [PubMed: 12239560]
21. Wallingford J, Harland R. Neural tube closure requires Dishevelled-dependent convergent extension of the midline. Development. 2002; 129:5815–5825. [PubMed: 12421719]
22. Jones C, Chen P. Bioessays. 2007; 29:120–132. [PubMed: 17226800]
23. Copp AJ, Checiu I, Henson JN. Developmental basis of severe neural tube defects in the loop-tail (Lp) mutant mouse: use of microsatellite DNA markers to identify embryonic genotype. Dev Biol. 1994; 165:20–29. [PubMed: 8088438]
24. Qian D, et al. Wnt5a functions in planar cell polarity regulation in mice. Dev Biol. 2007; 306:121–133. [PubMed: 17433286]
25. Kim J, et al. Biogenesis of gamma-secretase early in the secretory pathway. J Cell Biol. 2007; 179:951–963. [PubMed: 18056412]
26. Torban E, et al. Gene Expression Patterns. 2007; 7:346–354. [PubMed: 16962386]
27. Justice M, et al. Mamm Genome. 2000; 11:484–488. [PubMed: 10886010]
28. Justice MJ, Noveroske JK, Weber JS, Zheng B, Bradley A. Human Molecular Genetics. 1999; 8:1955–1963. [PubMed: 10469849]
29. Weber JS, Salinger A, Justice MJ. Genesis. 2000; 26:230–233. [PubMed: 10748459]
30. Wilson R, et al. The translocation, folding, assembly and redox-dependent degradation of secretory and membrane proteins in semi-permeabilized mammalian cells. Biochem J. 1995; 307(Pt 3):679–687. [PubMed: 7741697]
31. Kim J, Hamamoto S, Ravazzola M, Orci L, Schekman R. Uncoupled packaging of amyloid precursor protein and presenilin 1 into coat protein complex II vesicles. J Biol Chem. 2005; 280:7758–7768. [PubMed: 15623526]
32. Fromme J, et al. Developmental Cell, The Genetic Basis of a Craniofacial Disease Provides Insight into COPII Coat Assembly. 2007; 13:623–634.

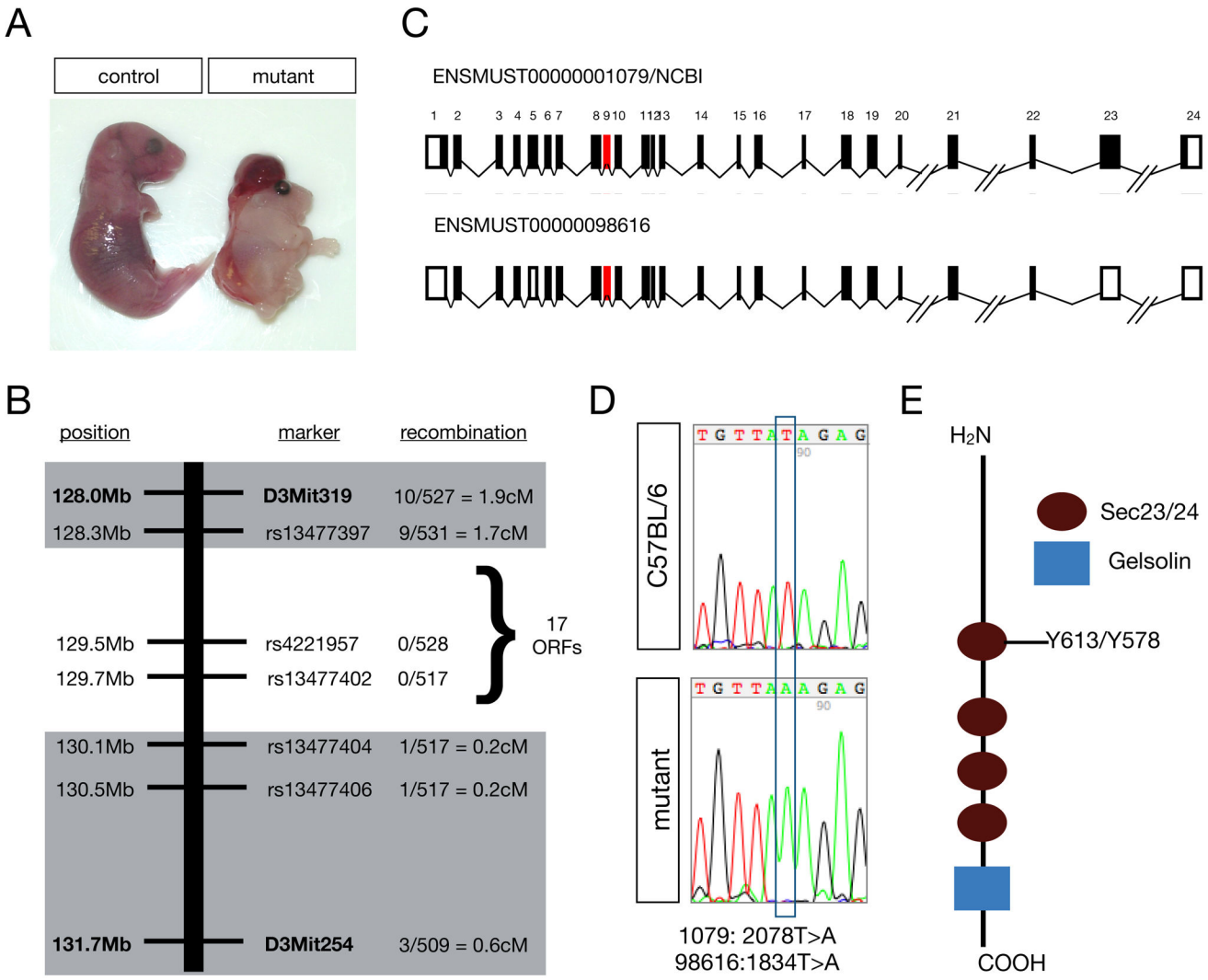

Figure 1. The mutation in mouse line 811 is Sec24b Y613

(A) Wholemount image of E18.5 811 mutant and control littermate showing the reduced size and craniorachischisis phenotype. (B) Schematic diagram of the region of chromosome 3 found to contain the 811 mutation, the markers used to diagnose linkage, and the frequency of recombination events observed at these markers. (C) Schematic diagram of the *Sec24b* genomic locus highlighting exon 9 (red) in which a single base pair substitution was observed. Shown in black are the coding exons from the two predicted transcripts, designated 1079 and 98616 generated from the mouse *Sec24b* locus (D) Sequence data highlighting the mutation *Sec24b* 1079: 2078T>A, 98616: 1834T>A observed in 811 mutants compared to C57BL/6 wildtype DNA. (E) Schematic diagram of Sec24b. The 811 point mutation introduces a stop codon within a Sec23/24 domain of Sec24b.

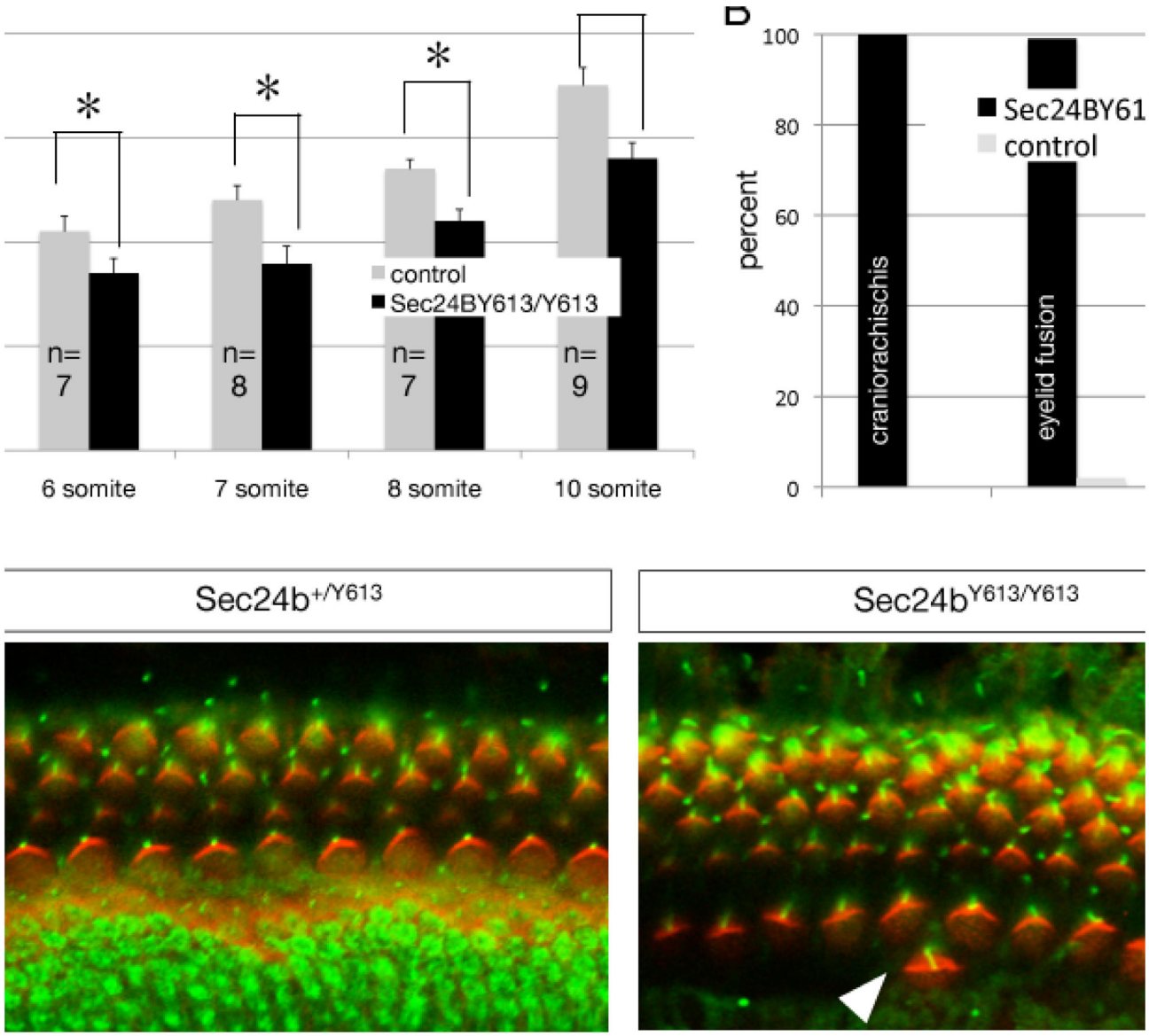

Figure 2. *Sec24b*$^{Y613/Y613}$ embryos have deficits in cochlear hair cell development and convergent extension

(A) *Sec24b*$^{Y613/Y613}$ mutants have deficits in convergent extension compared to *Sec24b*$^{+/Y613}$ and *Sec24b*$^{+/+}$ controls as assessed by the length:width ratio measured in 6-, 7-, 8-, and 10-somite staged E8.5 mutants. Mutants and controls from E8.5 litters were isolated and then binned based on somite number. The length and width of each embryo was then quantified, the length:width ratio calculated, the embryos were then genotyped and the length:width ratio compared between mutants and controls. n=7, 8, 7, 9 mutants and n=20, 18, 24, 28 controls at the 6-, 7-, 8-, and 10-somite stages, respectively (ANOVA, followed by Student Newman-Keuls, post hoc analysis *=p<0.01). (B) Frequency of craniorachischisis, eyelid fusion, and omphalocele observed in *Sec24b*$^{Y613/Y613}$ (n=38) mutants compared to littermate controls (n=166). (C) Wholemount immunohistochemistry

using acetylated-tubulin (green) and phalloidin (red) staining of E18.5 cochlea from *Sec24b*$^{Y613/Y613}$ mutants (n=10) and *Sec24b*$^{+/Y613}$ (n=10) controls. Arrowheads point to cells that have fallen out of phase. Scale bar in panel (C) is 10μM.

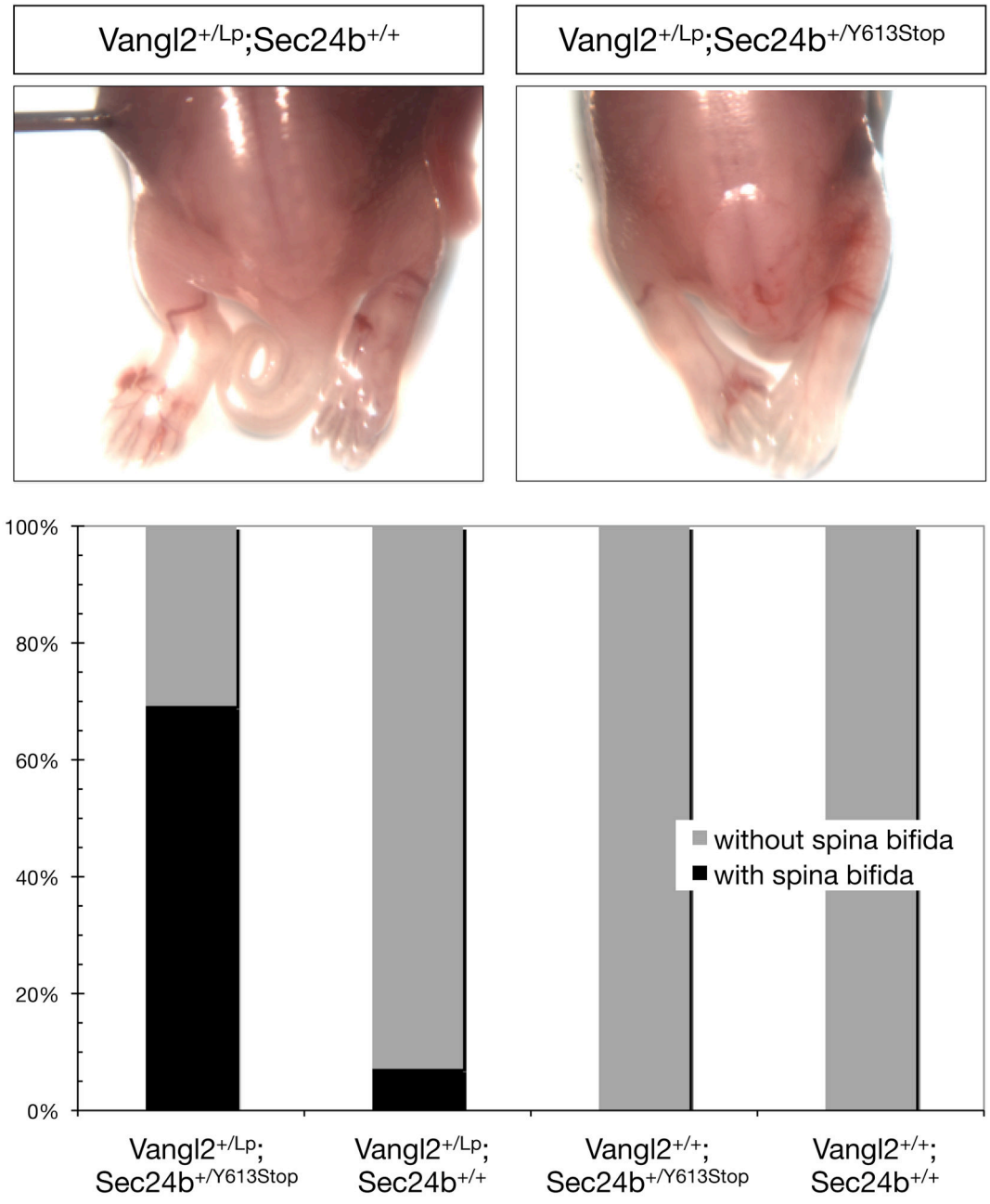

Figure 3. *Sec24b* and *Vangl2* genetically interact

(A) Posterior half of dorsal side up E16.5 embryos: *Vangl2*$^{+/LP}$; *Sec24b*$^{+/+}$ embryo (n=40) with proper neural tube closure and *Vangl2*$^{+/LP}$*; Sec24b*$^{+/Y613}$ transheterozygous embryo (n=18) with a posterior neural tube closure phenotype resembling spina bifida. (B) Quantification of the spina bifida phenotype penetrance in *Vangl2*$^{+/LP}$; *Sec24b*$^{+/Y613}$, *Vangl2*$^{+/LP}$; *Sec24b*$^{+/+}$, *Vangl2*$^{+/+}$; *Sec24b*$^{+/Y613}$, *and Vangl2*$^{+/+}$; *Sec24b*$^{+/+}$ embryos.

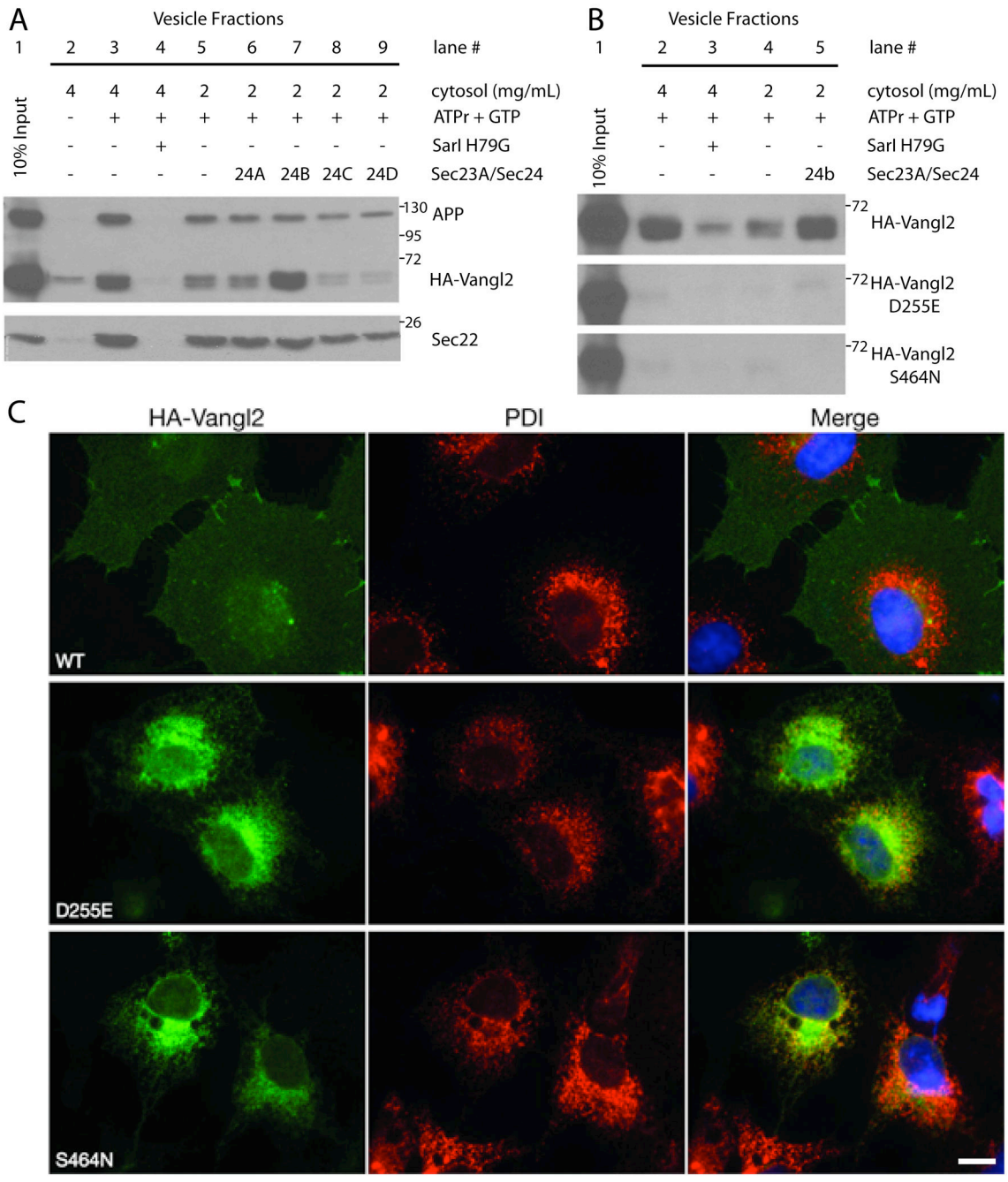

Figure 4. Sec24b strongly enhances the ER export of Vangl2 but not Vangl2 looptail mutants

(A) *In vitro* formation of COPII vesicles containing Vangl2. Donor (10% input, lane 1) membranes were incubated with rat liver cytosol. Strong productive budding of HA-Vangl2, APP, and Sec22 cargo proteins was detected at a cytosol concentration of 4mg/ml (lane 3) and reduced at 2mg/ml (lane 5). Excluding ATPr +GTP (lane 2) or addition of the dominant negative inhibitor of COPII budding, Sar1 H79G (lane 4), inhibited all three cargos from entering the vesicle fraction. Supplementing the lower concentration of cytosol with 10nM recombinant Sec23a/Sec24b (lane 7) strongly increased the degree to which HA-Vangl2

entered the COPII vesicles, but did not significantly affect the budding of APP or Sec22. Addition of the other recombinant Sec23a/Sec24 paralog combinations at the same 10nM concentration did not enhance the ability of HA-Vangl2 to enter vesicles (lanes 6, 8, and 9). (B) The ability of wildtype HA-Vangl2 to be packaged into COPII vesicles was compared to that of both Vangl2 mutant proteins, D255E and S464N. Wildtype Vangl2 entered the vesicle fraction in a COPII dependent manner and budding was enhanced by recombinant Sec23a/Sec24b (lanes 2-5). However, the single point mutations D255E or S464N completely blocked Vangl2 from entering COPII vesicles and leaving the ER. Positive control cargo proteins were packaged normally into COPII vesicles (Supplemental Figure 4) (C) Immunofluorescence staining of anti-HA (green) and anti-PDI (red) in COS7 cells. Transiently transfected wildtype HA-Vangl2 (WT) reached the cell surface, while both Vangl2 mutants D255E and S464N remain in the ER where they co-localize with the PDI ER marker. PDI=Protein Disulfide Isomerase, APP=Amyloid Precursor Protein, ATPr=ATP regenerating system. Images are representative of at least three independent experiments. Scale bar in panel (C) is 10μM.

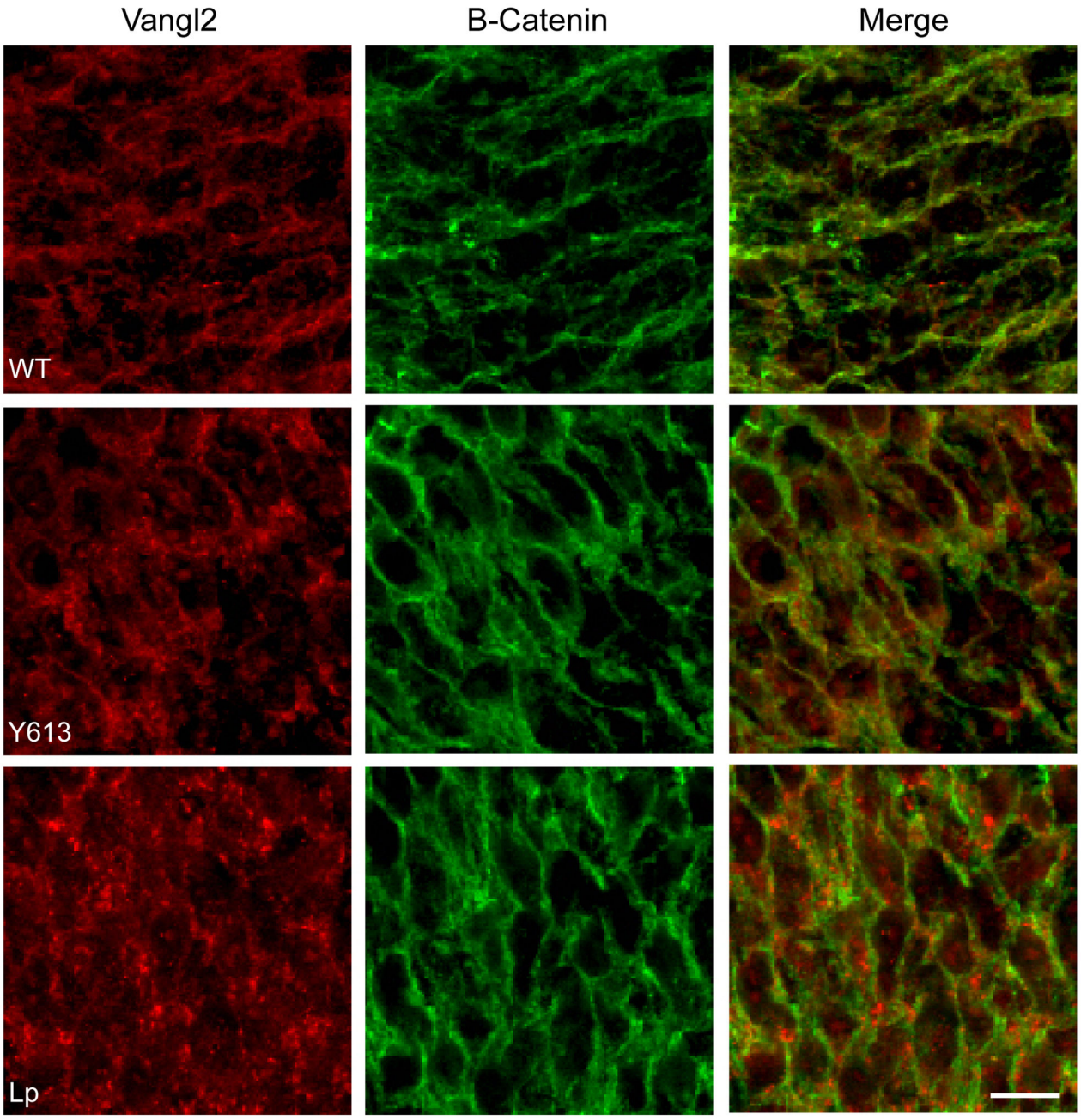

Figure 5. *Sec24b*$^{Y613/Y613}$ embryos show aberrant subcellular localization of Vangl2 in the developing spinal cord*in vivo*

Immunofluorescence staining shows colocalization of Vangl2 (red) and membrane bound Beta-Catenin (green) in the developing spinal cord of wildtype embryos. In contrast, developing spinal neuroepithelium of both Sec24$^{Y613/Y613}$ and *Vangl*$^{LP/LP}$ mutant embryos showed decreased Vangl2 membrane localization and increased intracellular puncta, while Beta-Catenin retained its membrane localization. Images are representative of three

independent experiments. Abbreviations: Y618, *Sec24b*$^{Y613/Y613}$; Lp, *Vangl2*$^{LP/LP}$. Scale bar is 10μM.